Functional screening of established and experimental weight loss drugs in terms of their effects on central dopamine release kinetics

A thesis submitted by

Rana T Alabdali

In partial fulfillment of the requirement for the degree of

Master of Science

In

Pharmacology and Drug Development

Tufts University

Sackler School of Graduate Biomedical Science

May 2018

Adviser: Emmanuel N Pothos, PhD

Abstract

One of the major causes for mortality and limitations on quality of living is obesity. The neurotransmitter dopamine plays a major role in obesity. Obese subjects have low D2 dopamine receptor availability and obese or obesity-prone animal models exhibit low mesolimbic dopamine release which potentially leads to hyperphagia as a compensatory mechanism. Our approach is that anti-obesity medications work on the dopamine pathway and correct this defect through direct or indirect mechanisms and that the efficacy of weight loss drugs should correlate with the correction of central dopamine systems. In the present study, we examine some medications such as topiramate (Topamax™) and an experimental N-Acylethanolamine Acid Amidase (NAAA) inhibitor to see if their mechanism in reducing weight is at least partly effected through the dopaminergic system in the brain. We use carbon fiber amperometry to examine dopamine release from the dorsal striatum in real time and compare it with baseline release. Topiramate showed a significant reduction in synaptic dopamine release. The NAAA inhibitor had the opposite effect. Further investigation is needed in order to understand the link between obesity and dopaminergic signaling pathway.

Acknowledgments

First of all, I would like to thank my sponsor Taif University for giving me this amazing opportunity to study abroad. Also, I would like to thank my mentor, Dr. Emmanuel Pothos for guiding me as a student in his lab and help me discovering more about Pharmacology and Neuroscience. He had always helped me with any difficulties that I had, and I learnt from him a lot of skills and techniques to improve my scientific acumen and empirical thinking. In addition, I would like to thank our collaborator, Dr. Efi Kokkotou, for giving me the opportunity to learn new experiences in her laboratory; and my parents who supported me through everything. Thank you everyone.

Table of Content

List of Tables:

List of Figures:

List of Abbreviations:

Artificial Cerebral Spinal Fluid (ACSF)

Area Under the Curve (AUC)

Body Mass Index (BMI)

N-Acylethanolamine Acid Amidase (NAAA)

Nucleus Accumbens (NAc)

Oleoylethanolamide (OEA)

Peroxisome Proliferation-Activated Receptor α (PPAR-α)

Reward Deficiency Syndrome (RDS)

Chapter 1: Introduction

Obesity is considered to be one of the main and important causes of morbidity, mortality, and limited life quality (1). There is more than thirty-five percent increase in the rate of obesity among adults in certain states in the United States (2). However, the central and peripheral mechanisms of weight gain are still unclear. There is apparently a link between obesity and the brain's dopaminergic pathway (3). Dopamine is a neurotransmitter that plays an important role in the food reward system (3). Moreover, a high body mass index (BMI) can affect dopamine receptors, mainly the D2 receptor. It has been shown that increasing body weight might decrease the availability of D2 receptors (4,5). Hyperphagia may be, partly, a compensation for this central dopaminergic deficit in order to avoid food craving (4,20). This hypothesis is also known as the Reward Deficiency Syndrome (RDS) (17), and this impairment can decrease dopaminergic functioning which may then result in abnormal eating behavior. Indeed, weight control medications are known to affect dopamine release through their action on D2 receptors (3). Therefore, we decided to pursue the overarching hypothesis that the efficacy of a weight loss drug may correlate with its direct or indirect effect on mesolimbic dopamine release even if its central mechanism of action is currently not well known.

An example of such a compound is oleoylethanolamide (OEA). It is an endogenous fatty acid amide, also considered to be an endocannabinoid-like lipid that induces hypoplasia and weight loss (24). It is released from the enterocytes and it acts as an agonist on the peroxisome proliferation-activated receptor α (PPAR-α). By activation of this receptor, OEA can suppress food intake through engaging with the vagal sensory afferents (21,22). It is also found that when OEA binds with PPAR-α, it activates the process of fat oxidation therefore increasing the energy production leading

to weight loss. Studies show that eating high fat diet continuously may decrease the anorexic signals of the OAE therefore more weight will be gained (23). In addition, OEA may reduce food intake depending on many factors including the dopaminergic reward pathway. It is suggested that OEA may enhance dopamine release, but the mechanism is still unclear (23,24,26). OEA is degraded and inactivated by a lysosomal enzyme called N-acylethanolamine acid amidase (NAAA), and this process take place in the macrophages (25). NAAA is present in many organs including intestine, lungs, thymus and spleen (27). NAAA inhibitors show protective effects against inflammation (29), hydrolyse anandamide and convert it to arachidonic acid (30). However, they have limited effects if administered orally (28). Topiramate blocks sodium and calcium channels (18) and may exert its effects on dopamine exocytosis through modulation of neuronal firing.

Our goal in this study is to assess the mechanism of topiramate and an experimental NAAA inhibitor as anti-obesity medications through their impact on the central dopaminergic system.

Chapter 2: Methods

2.1 Topiramate Project:

2.1.1 Animals for ex vivo testing:

8 weeks old C57BL6 black wild-type male mice were purchased from Jackson Laboratories and housed at the animal facility of Tufts University (Boston, MA) with a 12-hour light-dark cycle and regular lab chow diet.

2.1.2 Preparing the brain before slicing:

As per the laboratory's IACUC-approved protocol, I performed the following steps: place the artificial cerebral spinal fluid (ACSF) and sucrose-bicarbonate mix on ice (0 °C); placed the buffer tray, specimen disc, and the blade in the freezer (-20 °C); and added 100ml of oxygenated ACSF in a plastic chamber for tissue collection. After 20 minutes, I removed the buffer tray, specimen disc, and the blade from the freezer and put them on ice (0 °C). I used Loctite 404 Instant adhesive glue to attach a piece of agar to the specimen disc as a supportive base for the brain. Then, I euthanized the mouse with xylazyine and ketamine. I extracted the brain within less than 45 seconds post decapitation (9). I washed the brain with sucrose-bicarbonate reagent and cut the brain into two hemispheres and removed the cerebellum and some excess tissues around the brain. I placed each hemisphere of the brain on the agar base which I previously glued vertically with the specimen disc. The occipital lobe of the brain was glued to the disc whereas the prefrontal lobe was unattached on the opposite side.

2.1.3 Brain slicing with Vibratome:

I sliced the brain by using a Vibratome (Leica VT1000S). As per lab protocol, after placing the brain on the disc, I screwed the disc firmly, and added oxygenated ACSF to the buffer tray and adjusted the slicing process. Then, I sliced each brain tissue at a speed of 5.0 mm/s for a thickness of 300 µm and frequency of 7 Hz. Then, I

collected the sliced tissues into the oxygenated ACSF chamber. After finished slicing, we let the tissues rest in oxygenated ACFS chamber for at least one hour to let the brain tissues recover from cold shock.

2.1.4 Electrophysiology:

I prepared the electrophysiology microscope for recording as per the following steps. First, I turned on the computer software (Axograph Scientific Software, Berkeley, CA), the micromanipulator (Sutter Instrument Company MP-285), microelectrode amplifier (axon instruments 200b), pulse stimulator (Master-8 A.M.P.I), electrophysiology microscope, temperature controller (Warner Instruments Corporation TC-324B), stimulus isolator (Iso-Flex A.M.P.I Model 4100), suction vacuum, and the oxygen supply. After turning on all the required devices, I placed an ACSF bottle on top of the electrophysiology cage and inserted into the bottle a micro tube line end for the oxygen supply for the ACSF, and a grounding wire from the electrode stage into the slice bath to reduce noise. I flushed the tubes with 10-15 ml of Nanopure water to remove any prior solutions. Slices from the dorsal striatum, one at a time, were placed in the middle of the slice bath holder that was supported with magnets and supplied the brain tissue with oxygenated ACSF, suction, and grounding wire. The flow of ACSF to the brain slice was continuous and constant at 1 cc per minute. In addition, I filled the recording electrode with concentrated Potassium Chloride and inserted it inside its holder found in the left arm of this electrophysiology microscope. The right arm held the stimulating bipolar electrode (Plastics One). After I adjusted the flow and the electrodes, I placed the desired brain tissue in the middle of the bath which is placed under the lens of the upright Olympus microscope and secured with a mesh cover. Then, I slided the whole microscope stage under the microscope lens and let the lens submerge in the ACSF liquid. After that, I adjusted the focus of the lens on the striatum region and merged the two electrodes into the ACSF liquid. The recording electrode was placed between the

two poles of the stimulating electrode (without touching). For recording the baseline, I acquired through Axograph for five seconds before the electrical stimulation of the slice. with 5 nA of electric current. The recording lasted for twenty seconds post stimulation. The trace was filtered through low-pass Gaussian filter and set it 1 kHz. Slice rested for 5 min for recovery. I stimulated each slice 5 times.

2.1.5 Topiramate treatment:

Topiramate (Topamax 25mg film-coated tablets, Janssen 2016) was applied at a dose of 0.7 ug/ml. A dose of 200 mg topiramate in humans is found to have a median CSF concentration of 14.28 umol/L as total (free + unbound) (10), while the calculated concentration for brain tissue would be around 2 umol/L (conversion factor 2.95) (11). For the present study, I dissolved 25mg in 1 liter of demethylsulfoxide (DMSO) and prepared x100 stock solution aliquots stored in -20 °C. For the solution applied in the slice bath, I dissolved the aliquot in 100ml ACSF (12) and applied it at rate of 1 cc for 30 minutes, then delivered the five electrical stimulations delivered above to each slice.

2.2 NAAA inhibitor project:

2.2.1 Animals:

20 weeks old black C57BL/6 male mice were purchased from Charles River Laboratory (USA).Their average body weight was 27.68g. Each mouse was housed alone in a single cage.

2.2.2 Animal selection:

Mice were randomized into two groups; both groups consisted of 10 animals. Each animal was identified by an ear tagged individual number. A cage card was used to identify each cage and was marked with the treatment group number and animal number.

2.2.3 NAAA inhibitor preparation:

N-Acylethanolamine hydrolyzing acid amidase (NAAA) inhibitor (AM11095), synthesized at Northeastern University, was prepared as per Alhouayek et al (FASEB 2015). Briefly, 30 mg of drug was first dissolved in DMSO (20 ul), the add equal amount of ethanol, further diluted in salient of 20 ml and vortexed to make a suspension. The suspension was mixed well before intraperitoneal administration of the suspension and salient solution was used as vehicle control.

2.2.4 Experimental design:

Twenty mice were divided into two groups, ten for the NAAA inhibitor treatment and ten for the vehicle (control) group. All the mice were fed with HFD for 4 days before the experiment. On day 0, each mouse received intraperitoneal injection (i.p.) daily either with AM11095 NAAA inhibitor suspension for a dose of 10 mg/kg and a total a volume of (200 ul) daily or received a vehicle for the control group. Based on weight changes, on day 4, the dose was increased to 15 mg/kg as a total volume of (300 ul) for the NAAA inhibitor group and the control group for another 4 days. Then the dose was increased to 20 mg/kg of total volume of (400 ul) for the NAAA inhibitor group and the control group for another 7 days. During the experiment, mice weight, food intake, mice survival was measured daily before and after treatment. At the end of the experiment, the animals were processed for slice electrophysiology.

Group	No. of Animals	Treatment	Time (days)	Treatment	Time (days)	Treatment	Time (days)
1	10 males	200 ul Vehicle	4	300 ul Vehicle	4	400 ul Vehicle	7
2	10 males	200 ul AM11095	4	300 ul AM11095	4	400 ul AM11095	7

TABLE 2.1: Experimental design for the NAAA inhibitor incremental treatments and the vehicle groups.

Chapter 3: Results

3.1 Electrophysiology analysis:

3.1.1 Topiramate data analysis:

3.1.1.1 Amplitude: After analyzing the data through Axograph, topiramate bath application for 30 min induced significant reduction in the dopamine peak amplitudes (heights) as when compared with ACSF bath (baseline) dopamine peak amplitudes. The amplitude represents the highest efflux of dopamine release from baseline after stimulation (8). The mean dopamine amplitude for the baseline peak was 185.1 ± 34.2 (± SEM) picoAmber (pA) and the mean dopamine amplitude for topiramate treated was 80.6 ± 22.72 pA. The minimum basic dopamine amplitude was 0.40 pA and the minimum dopamine amplitude for the topiramate was 0 pA. Furthermore, the maximum basic peak amplitude was 2083 pA and the maximum dopamine amplitude for the topiramate was 1218 pA.

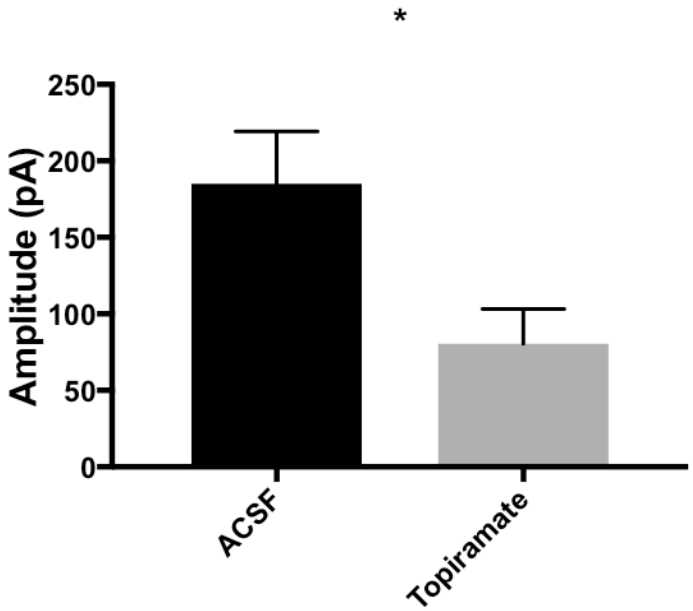

Figure 3.1: The amplitude of elrectrically evoked dopamine in ACSF versus topiramate-bathed striatal slices (mean ± SEM). * P =0.0128, paired t-test, N=13.

3.1.1.2 Width: Topiramate bath application showed a significant reduction in the width of electrically evoked dopamine events, which represents the period of between the onset of dopamine release until the end point of the event before it drops back to baseline. The mean dopamine width for the baseline (ACSF bath) was 2.17 ± 0.31 (± SEM) milliseconds (ms) and for the topiramate bath was reduced to 0.55 ± 0.09 ms.

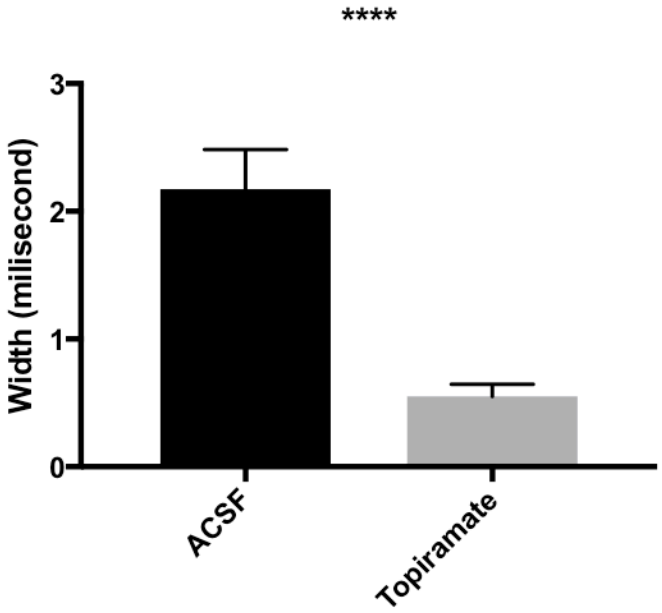

Figure 3.2: The width of dopamine in ACSF versus Topiramate bath application. ****P<0.0001, paired t-test, N=13.

3.1.1.3 Dopamine Molecules Released per Event: The dopamine molecule number was derived through calculating the Area Under the Curve (AUC) and converting it through the use of Faraday's equation (31);

$$N = \frac{A \int_{t1}^{t2} I \, dt}{n.F}$$

Where, A = 6.2 x 10^{23}, F= 96,485, n= 2 (the number of electrons transferred with each neurotransmitter molecule), t1= the first onset time of signal rise from baseline, and t2= the end time the signal reached baseline after t1. The mean dopamine molecules per event in ACSF were 273,661,881 ± 47,625,098 (± SEM) pA.ms and the mean dopamine molecules for the topiramate bath application were 236,113,889 ± 129,864,121 pA.ms.

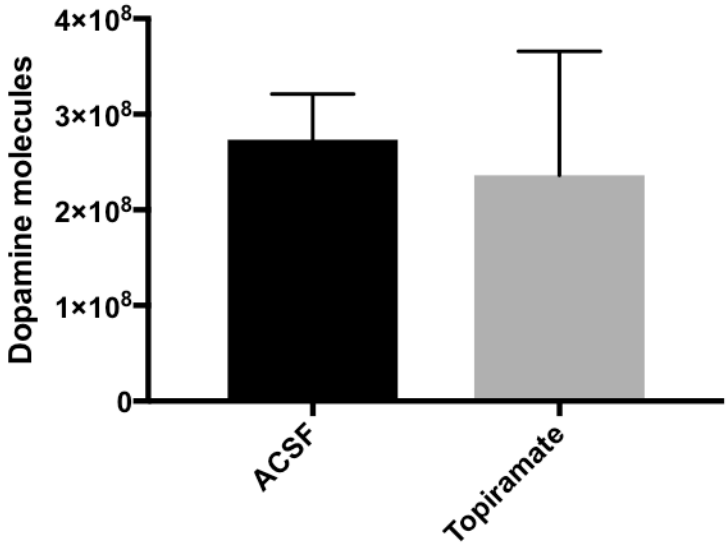

Figure 3.3: The dopamine molecules per electrically evoked event in ACSF versus Topiramate baths. P =0.7862, paired t-test, N=13.

3.1.2 NAAA inhibitor data analysis:

3.1.2.1 Amplitude: Treatment with the NAAA inhibitor induced significant amplification in the dopamine peak amplitudes in striatal slices when compared with the control mice. The mean dopamine amplitude for the control group was 5.61 ± 1.54 (± SEM) nanoAmber (nA) and the mean dopamine amplitude for the NAAA inhibitor treated group was 14.85 ± 0.8 nA.

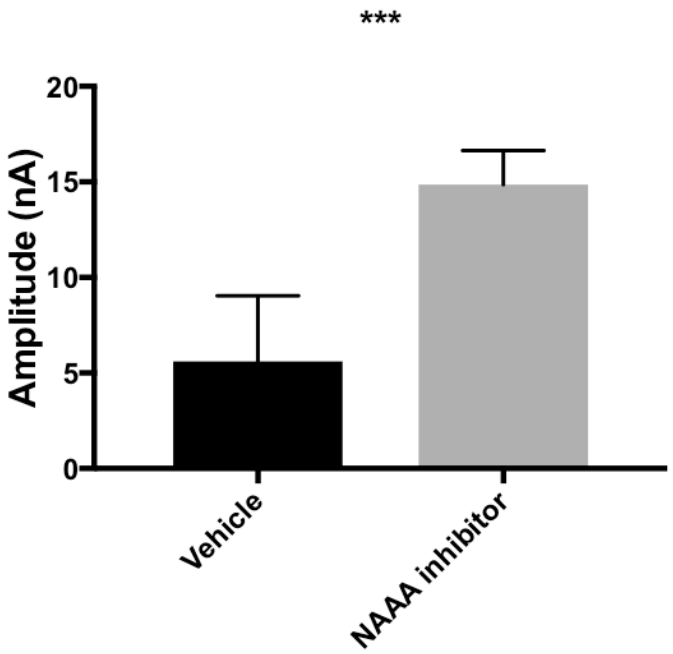

Figure 3.4: The dopamine amplitude in vehicle versus NAAA inhibitor treated mice. * P <0.0007, paired t-test and error bar represent 95% CI and mean ± SER, N=2 per group.

3.1.2.2 Width: Mean dopamine width for the vehicle group was 5.46 ± 1.67 milliseconds (ms) versus 18.3 ± 0.86 ms for the NAAA inhibitor group.

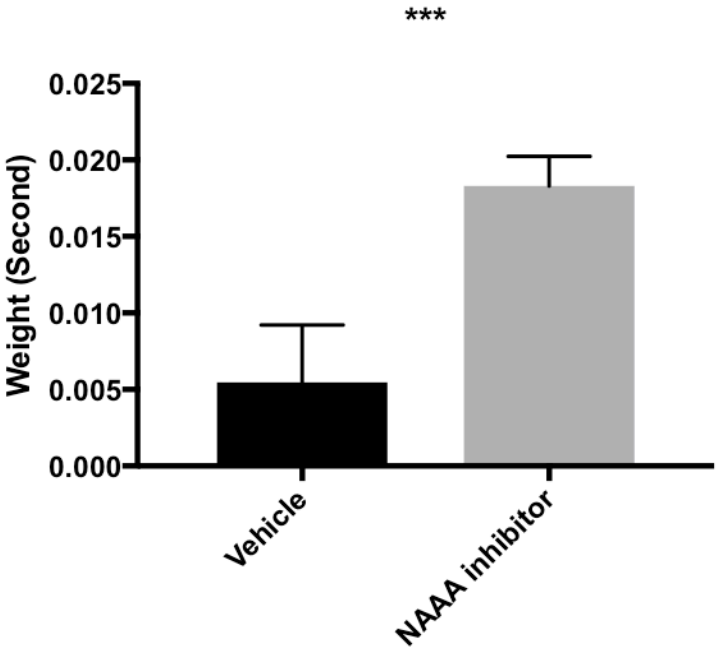

Figure 3.5: The dopamine width in baseline release verses NAAA inhibitor release. * P <0.0001, paired t-test and error bar represent 95% CI and mean ± SEM, N=2 per group.

3.1.2.3 Dopamine Molecules per Event: Mean dopamine molecules released per event in the vehicle group were 10,293 ± 4,243 nA.s versus 74,542 ± 3,543 nA.s for the NAAA inhibitor.

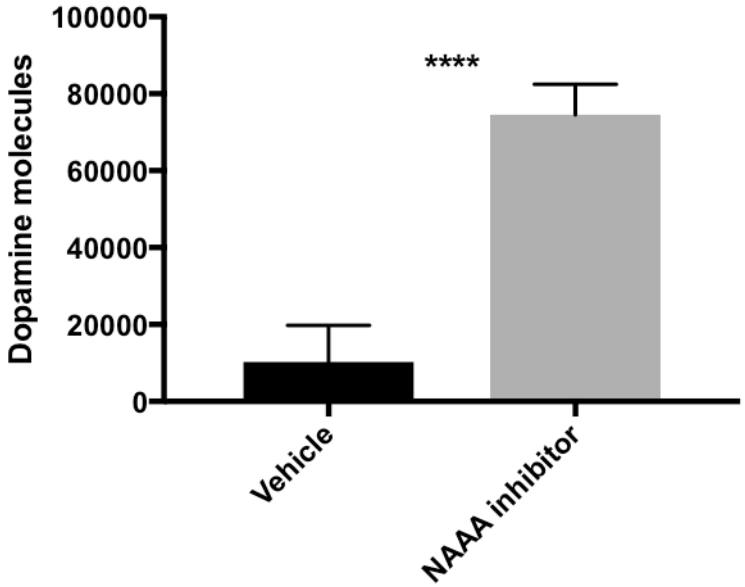

Figure 3.6: Evoked dopamine molecules per event in vehicle versus NAAA inhibitor treated mice. **** P <0.0001, paired t-test, N=2 per group.

3.2 Weight and food intake analysis:

3.2.1 Body Weight and Food Intake

A small weight loss (2%), calculated as a percentage of the start weight on Day 0 of treatment, was observed in NAAA inhibitor treated groups. With the increase in the NAAA inhibitor dose, the mouse body weight loss did not increase. This evidence might indicate that after administration of NAAA inhibitor, animal body weight was transiently reduced and recovered or adapted to the presence of this inhibitor. The daily consumption of high fat diets was also examined. There was no statistically significant difference on food intake between NAAA inhibitor treated and vehicle treated mice

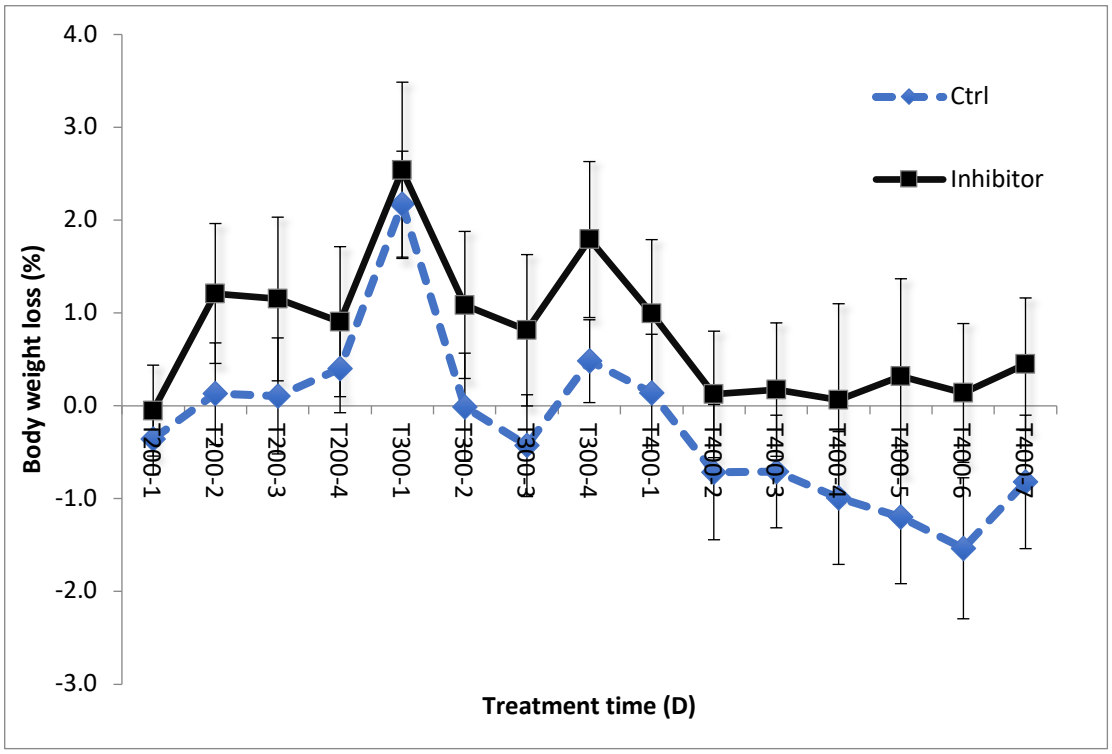

Figure 3.7: The body weight loss percentage in vehicle (Ctrl) group versus NAAA inhibitor group (n=10 mice per group).

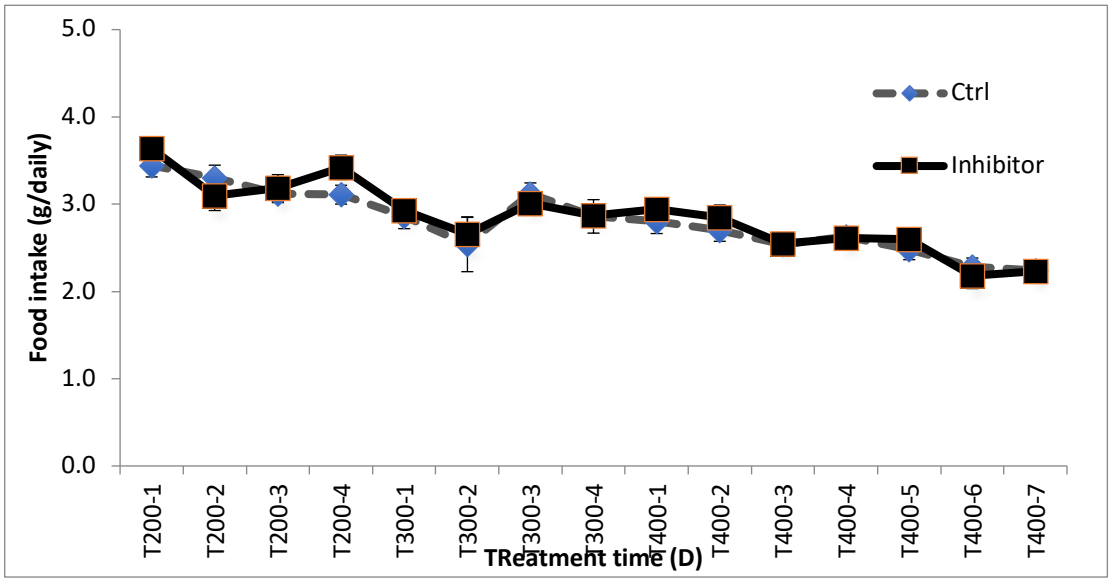

Figure 3.8: No statistically significant differences in HFD intake were observed between vehicle and NAAA inhibitor treated mice (n=10 mice per group).

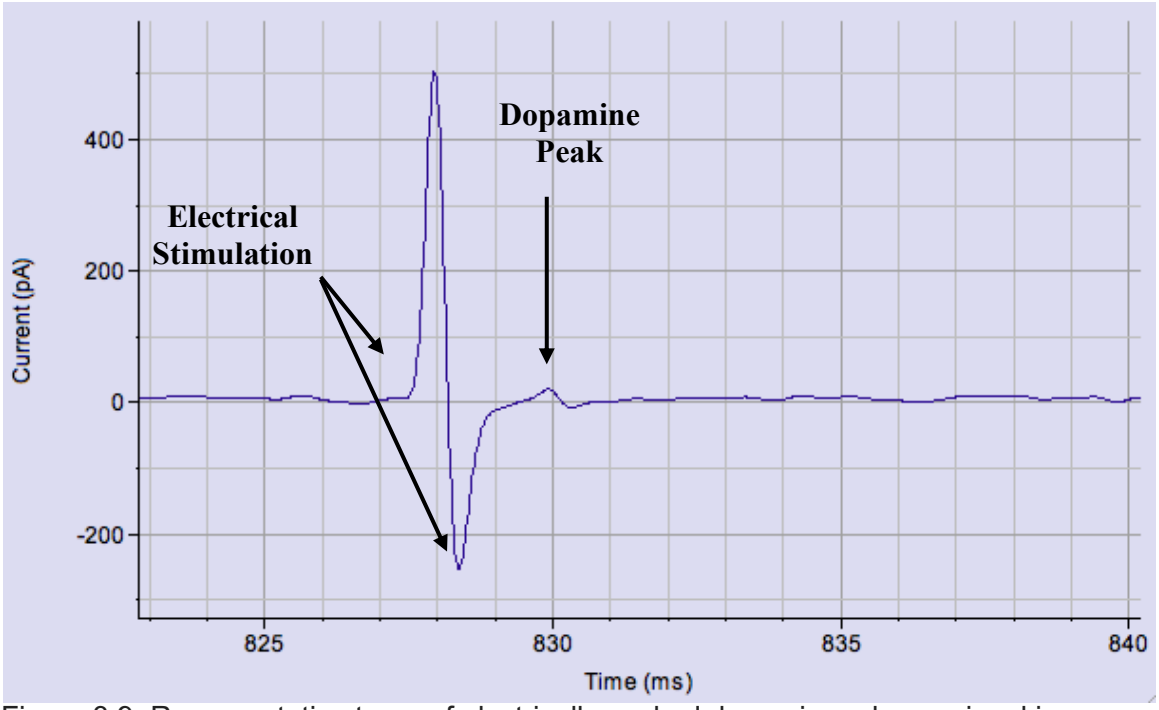

Figure 3.9: Representative trace of electrically evoked dopamine release signal in topiramate bath from a striatal slice showed limited dopamine release

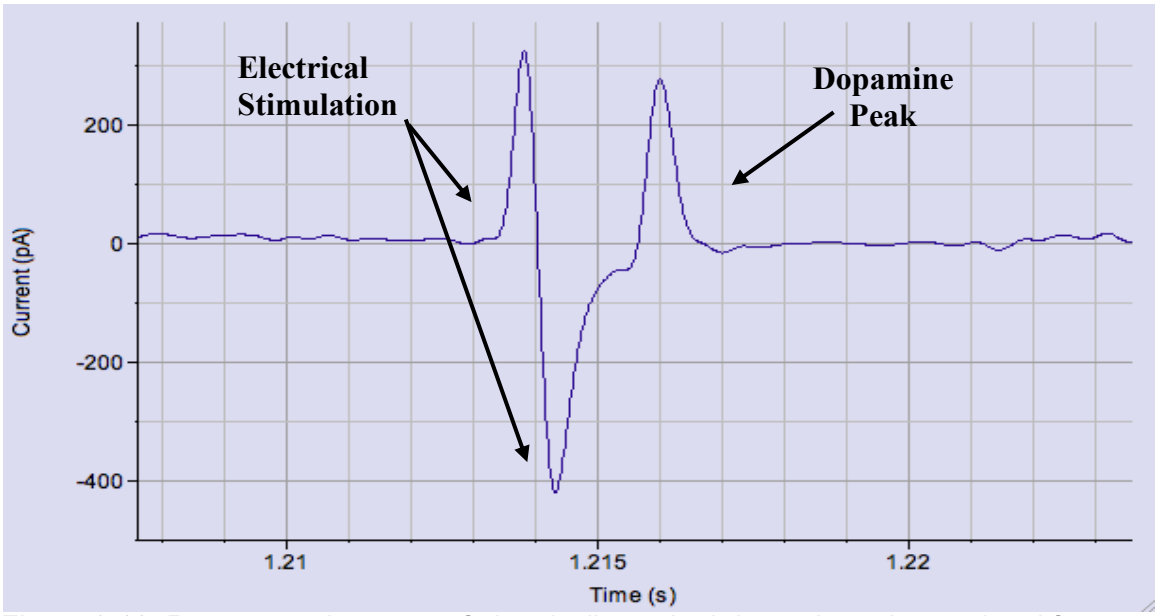

Figure 3.10: Representative trace of electrically evoked dopamine release signal from a striatal slice of an NAAA inhibitor treated mice

Chapter 4: Discussion

Our preliminary studies on functional screening of two weight loss drugs, an established drug like topiramate and a candidate drug like an NAAA inhibitor showed that the effects of such drugs on central dopamine kinetics may potentially constitute an underlying criterion for the assessment of their efficacy.

Topiramate at a pharmacologically relevant bath application for 30 minutes was found to induce a decrease in evoked striatal dopamine signal amplitude and width, although the small number of slices tested contributed in not establishing so far a statistically significant decrease in the number of dopamine molecules released per event. However, this pilot experiment was done without assessing the effects of chronic and systemic topiramate on body weight. The difference in the amplitude and the width may suggest that topiramate might partially affect the dopamine reuptake process in the striatum region. Some studies showed that topiramate has decreased dopamine in the nucleus accumbens (NAc) in alcohol use disorder (32). Furthermore, it may inhibit the dopamine function in the cortico-mesolimbic area (33). Other clinical data showed that dopamine agonist drugs that are used for Parkinson disease are causing actual weight gaining; one example of such compounds is Pramipexole (34,35). Another dopamine agonist, L-dopa, which is also used for Parkinson disease, have shown a long-term weight gaining in a group of treated mice compared with vehicle mice (6). In addition, downregulation of the D2 receptor may lead to increase extracellular dopamine level in case of obesity (15-16). So, topiramate could decrease weight by partially attenuating dopamine release and reducing food intake, although this remains to be tested in our studies.

The NAAA inhibitor could act through attenuating the degradation of oleoylethanolamide and increasing its levels. In our hands, even a small 2 % weight loss was accompanied by a significant increase in evoked dopamine signal in the

striatum of the NAAA inhibitor AM11095-treated mice. There was little but trending difference on weight loss and HFD intake when escalating the NAAA inhibitor dose. Previous studies have shown that NAAA inhibitors are anti- inflammatory drugs (7) and inhibit inflammasomes (13,14,36). These effects could relate to the activation of the dopaminergic pathway signaling. AM11095 may act as a dopamine agonist which may bind to dopamine receptors or it may activate dopamine exocytosis from vesicles.

In conclusion, we are at the very beginning steps of establishing a new functional assay of weight loss drugs whereby the metabolic profile of each drug candidate will be assessed vis a vie its effect on central and site-specific neurotransmitter kinetics in real time followed by a cprrelation analysis between drug efficacy and the spectrum of central effects. Such assays can eventually lead to the establishment of advanced criteria for the prediction of efficacy of new weight loss drugs.

Chapter 5: Appendix

5.1 Constructing and testing carbon fiber amperometric electrodes:

As per lab's protocol, we follow eight steps for the construction of recording microelectrodes in house:

Step 1: Pull in the Carbon Fiber

a) From a set of carbon fibers, isolate a single fiber.
b) Using a vacuum, draw in a glass capillary filament of 1.0MM x 0.58 mm (or .75 mm) x 4.0".
c) While holding down one end of the fiber, draw the fiber into the capillary so that the fiber sticks out at both ends of the capillary.
d) Verify with an incandescent light microscope at a low magnification (10X) that one fiber end sticks out of each side of the capillary tube.

Step 2: Pull Capillaries

a) Using a flaming/brown micro pipette puller (Model P-97 from Sutter Instrument Company) at #53 setting, place capillary in holder by bringing the capillary tube through the heating element gently in order not to break the heating filament and slowly tightening the nozzles for each holder alternating between each to evenly distribute tightened grip on the capillary.
b) Push the green pull button.
c) Once the capillary is split in half, use scissors to cut the melted capillary point at the instance where it exits the heating mechanism.
d) Remove the partly finished electrode and place in a safe holder with the electrode lying horizontally attached on a double-sided adhesive tape (vertically stored electrodes can easily break).

Step 3: Cut

a) Check electrodes under a 10x mag microscope at the point in which the fused glass begins to thicken.
b) Place electrode in a safe place.

Step 4: Glue

a) With electrodes prepared, the carbon fibers were fixated to the glass tube with an Epoxy resin/hardener. Mix the part A to part B Epoxy, in a ratio of 4:1, respectively.
b) Hold the tip ends in the glue for two minutes and then place electrodes in a standing holder that can go in an oven at 65°FC.

Step 5: Bake

a) Place electrodes in the incubator for 3 hours at 65°C.
b) Let the electrodes cool overnight.

Step 6: Bevel

a) Place the electrode in the holder of the K.T. Brown Type micro-pipette beveller model BV-10 (Sutter Instrument Company) so that it is at a 40-degrees angle and locate the electrode tip under the light microscope.
b) Turn on the rotating platform. Make sure the surface is properly lubricated by squirting Nanopure water when necessary.
c) Gently lower the electrode to the rotating platform so that the tip touches the surface and let it sit for five to seven minutes adding more water when necessary.
d) Under the microscope check the tip edge of the electrode to make sure it has a slanted edge.

Step 7: Testing

a) Set up the microscope for electrophysiology using the MP-285 Micromanipulator (Sutter Instrument Company), the platform of the Nikon Inverted Microscope Eclipse TE300, the Axopatch 200B Integrating Patch Clamp (by Axon Instruments Inc.) set at 700 mV, and an Apple MacBook Pro with AxoGraph X software.
b) Fill the electrode with potassium chloride, KCl, use a MicroFil tip syringe and place in holder on stage of microscope. Ensure there are no air bubbles in the electrode by slowly pulling the MicroFil out of the electrode.
c) Fill a small dish with ACSF and place under microscope.
d) Lower the electrode to the surface of the ACSF using reflection of ACSF surface and vision.
e) Place in the ACSF the ground electrode and check the electrode isn't overloaded and the RMS value doesn't exceed 3.5.
f) Turn on the Axograph to a blank page. Do not save anything.
g) Press start and wait 5 seconds to place a dopamine 100 ul drop next to the electrode into the petri dish.

Step 8: Preserve the Electrode

a) Remove electrode and fill electrode with Nanopure water using the syringe with the MicroFil tip. Then wash the electrode and holder in Nanopure water and place the electrode in order electrodes from good to poor quality.
b) Label electrodes to keep a record of them.

5.2 Reagents and solutions:

5.2.1 Artificial Cerebral Spinal Fluid (ACSF) Solution:

Reagents *	g/500mL	g/L	g/2L
NaCl (mw 58.44)	3.623	7.247	14.494
KCl (mw 74.55)	0.075	0.149	0.298
KH2PO4 (mw 136.1)	0.085	0.170	0.340
MgSO4 (mw 120.4) **or** MgSO4* 7H2O (mw 246.5)	0.120 **or** 0.247	0.241 **or** 0.493	0.482 **or** 0.986
NaHCO3 (mw 84.1)	1.051	2.103	4.206
CaCl2 (mw 111.0)	0.111	0.222	0.444
Glucose (mw 180.2)	0.911	1.982	3.964

Table 5.1: reagents for Arificial Spinal Fluid. *All reagents from Sigma-Aldrich, St. Louis, MO.

5.2.2 Potassium Chloride Solution:

Reagents *	g/L
NaCl (mw 58.44)	3.647
KCl (mw 74.55)	5.964
Hepes (mw 238.30)	2.384
CaCl2 (mw 111.0)	0.666
MgCl2 (mw 95.21)	0.204
NaH2PO4 * H2O (mw 138.0)	0.120
Glucose (mw 180.2)	4.506

Table 5.2: Potassium Chloride Solution. *All reagents from Sigma-Aldrich, St. Louis, MO.

5.2.3 Sucrose-Bicarbonate Solution:

5.2.3.1 Sucrose Solution:

Reagents *	g/L	g/2L
Sucrose (mw 342)	574.56	1436.4
KCl (mw 74.6)	2.61	5.22
CaCl2 * 2H2O (mw 147)	1.47	2.94
MgCl2 * 6H2O (mw 203)	8.12	16.24
NaH2PO4 * H2O (mw 138)	1.72	3.44
Glucose (mw 180)	18	36

Table 5.3: Sucrose Solution. *All reagents from Sigma-Aldrich, St. Louis, MO.

First, I filled a graduated cylinder with 50% of desired volume with Nanopure water and placed magnetic stir bar inside at stir at 4/10 (Corning, Hot Plate/Stirrer). Individually weighed each reagent and the Sucrose was added gradually. After adding each reagent, I washed and filled the cylinder with the remaining 50% of Nanopure water. I waited till everything was dissolved. Then, I filtered the solution with disposable sterile vacuum filter, 0.22 um pore size CN membrane (Corning, product #430186, NY) and labeled and stored it in cold room 8°C.

5.2.3.2 Sodium Bicarbonate Solution:

Reagents*	g/L
NaHCO3 (mw 84)	21.84

Table 5.4: Sodium Bicarbonate Solution. *All reagents from Sigma-Aldrich, St. Louis, MO.

5.2.4 Agar 1% Base:

First, I filled a beaker with 500 ml of Nanopure water and added magnetic stir bar and turned the heater on 5/10 (Corning, Hot Plate/Stirrer). Then, I weighted 5 grams of Agarose type 1-B, low EEO (Sigma, MO). Allowed the water to boil, then slowly I added the agar powder and turned the stir up to 7-8. When the solution turned transparent, then I removed the beaker immediately and poured the agar solution into dishes size 35mm x 10mm style (Corning, NY). Then, I allowed the dishes to solidify at room temperature, after that I capped and wrapped the dishes with Parafilm M (American National Can, IL) and stored them in cold room 8°C. (all reagents from Sigma-Aldrich, St. Louis, MO).

5.2.5 Dopamine solution:

Reagents*	Amount
Perchloric Acid 70% (0.3N) (mw 100.46)	0.3 ml
Dopamine HCL (mw 189.64)	1mg/ml

Table 5.5: Dopamine Solution. *All reagents from Sigma-Aldrich, St. Louis, MO.

References

(1) Abdelaal, Mahmoud, et al. “Morbidity and Mortality Associated with Obesity.” Annals of Translational Medicine, AME Publishing Company, Apr. 2017, www.ncbi.nlm.nih.gov/pmc/articles/PMC5401682/.

(2) “Obesity Rates & Trends.” Obesity Rates & Trends - The State of Obesity, stateofobesity.org/rates/.

(3) Wang, Gene-Jack. “Brain Dopamine and Obesity.” The Lancet, Elsevier, 6 Feb. 2001, www.sciencedirect.com/science/article/pii/S0140673600036436.

(4) Volkow, N D, et al. “Reward, Dopamine and the Control of Food Intake: Implications for Obesity.” Trends in Cognitive Sciences., U.S. National Library of Medicine, Jan. 2011, www.ncbi.nlm.nih.gov/pubmed/21109477.

(5) Benton, D, and H A Young. “A Meta-Analysis of the Relationship between Brain Dopamine Receptors and Obesity: a Matter of Changes in Behavior Rather than Food Addiction?” International Journal of Obesity (2005)., U.S. National Library of Medicine, Mar. 2016, www.ncbi.nlm.nih.gov/pubmed/27001642.

(6) Reinholz, J., Skopp, O., Breitenstein, C., Bohr, I., Winterhoff, H., & Knecht, S. (2008, December 1). Compensatory weight gain due to dopaminergic hypofunction: New evidence and own incidental observations. Retrieved March 26, 2018, from https://www.ncbi.nlm.nih.gov/pmc/articles/PMC2615020/

(7) Solorzano, C., Zhu, C., Battista, N., Astarita, G., Lodola, A., Rivara, S., . . . Piomelli, D. (2009, December 08). Selective N-acylethanolamine-hydrolyzing acid amidase inhibition reveals a key role for endogenous palmitoylethanolamide in inflammation. Retrieved March 27, 2018, from https://www.ncbi.nlm.nih.gov/pmc/articles/PMC2791595/

(8) Chang, X., Shirazian, A., Cai, W., Kahn, C., & Pothos, E. (2016, April 3). The Role of Central Insulin Resistance in Neuronal Synaptic Plasticity Associated with Neuropsychiatric Disorders. Retrieved March 27, 2018, from https://www.endocrine.org/meetings/endo-annual-meetings/abstract-details?ID=27251

(9) Segev, A., Garcia-Oscos, F., & Kourrich, S. (2016, June 15). Whole-cell Patch-clamp Recordings in Brain Slices | Protocol. Retrieved January 18, 2018, from https://www.jove.com/video/54024/whole-cell-patch-clamp-recordings-in-brain-slices

(10) Christensen, J., Højskov, C. S., Dam, M., & Poulsen, J. H. (2001). Plasma Concentration of Topiramate Correlates With Cerebrospinal Fluid Concentration. Therapeutic Drug Monitoring,23(5), 529-535. doi:10.1097/00007691-200110000-00006

(11) Patsalos, P. N., and Blaise F. D. Bourgeois. The Epilepsy Prescriber's Guide to Antiepileptic Drugs. Cambridge University Press, 2010.

(12) Baskys, A., Segal, J., & Fang, L. (2002). Neuroprotective properties of topiramate in organotypic hippocampal cultures: implications for treatment of vascular and other dementias. Drug Development Research,56(3), 393-400. doi:10.1002/ddr.10091

(13) Hwang, J. S., An, J. M., Cho, H., Lee, S. H., Park, J. H., & Han, I. O. (2015, January 05). A dopamine-alpha-lipoic acid hybridization compound and its acetylated form inhibit LPS-mediated inflammation. Retrieved March 30, 2018, from https://www.ncbi.nlm.nih.gov/pubmed/25445046

(14) Zhang, X., Liu, Q., Liao, Q., & Zhao, Y. (2017, August 25). Potential Roles of Peripheral Dopamine in Tumor Immunity. Retrieved March 30, 2018, from https://www.ncbi.nlm.nih.gov/pubmed/28928888

(15) Narayanaswami, V., Thompson, A. C., Cassis, L. A., Bardo, M. T., & Dwoskin, L. P. (2013, August). Diet-induced obesity: dopamine transporter function, impulsivity and motivation. Retrieved February 24, 2018, from https://www.ncbi.nlm.nih.gov/pubmed/23164701

(16) Narayanaswami, V., Thompson, A. C., Cassis, L. A., Bardo, M. T., & Dwoskin, L. P. (2013, August). Diet-induced obesity: dopamine transporter function, impulsivity and motivation. Retrieved February 24, 2018, from https://www.ncbi.nlm.nih.gov/pubmed/23164701

(17) Blum, K., Thanos, P. K., & Gold, M. S. (2014, September 17). Dopamine and glucose, obesity, and reward deficiency syndrome. Retrieved February 24, 2018, from https://www.ncbi.nlm.nih.gov/pmc/articles/PMC4166230/

(18) Naegel, S., & Obermann, M. (2010, February 3). Topiramate in the prevention and treatment of migraine: efficacy, safety and patient preference. Retrieved February 27, 2018, from https://www.ncbi.nlm.nih.gov/pmc/articles/PMC2951059/

(19) Lasley, E. N. (2008, September). New Treatments for Alcoholism Show Promise . Retrieved February 27, 2018, from http://www.dana.org/Publications/Brainwork/Details.aspx?id=43747

(20) Geiger, B. M., Haburcak, M., Avena, N. M., Moyer, M. C., Hoebel, B. G., & Pothos, E. N. (2009, April 10). Deficits of mesolimbic dopamine neurotransmission in rat dietary obesity. Retrieved March 01, 2018, from https://www.ncbi.nlm.nih.gov/pubmed/19409204

(21) Provensi, G., Coccurello, R., Umehara, H., Munari, L., Giacovazzo, G., Galeotti, N., . . . Passani, M. B. (2014, August 05). Satiety factor oleoylethanolamide recruits the brain histaminergic system to inhibit food intake. Retrieved March 01, 2018, from http://www.pnas.org/content/111/31/11527

(22) Hankir, M. K., Seyfried, F., Hintschich, C. A., Diep, T. A., Kleberg, K., Kranz, M., . . . Fenske, W. K. (2017, February 07). Gastric Bypass Surgery Recruits a Gut PPAR-α-Striatal D1R Pathway to Reduce Fat Appetite in Obese Rats. Retrieved March 01, 2018, from https://www.ncbi.nlm.nih.gov/pubmed/28065827

(23) Sihag, J., & Jones, P. J. (2017, November 10). Oleoylethanolamide: The role of a bioactive lipid amide in modulating eating behaviour. Retrieved March 01, 2018, from http://onlinelibrary.wiley.com/doi/10.1111/obr.12630/full

(24) Oleoylethanolamide: A fat ally in the fight against obesity. (2017, February 27). Retrieved March 01, 2018, from https://www.sciencedirect.com/science/article/pii/S0031938416311994

(25) Antinociceptive effects of the N-acylethanolamine acid amidase inhibitor ARN077 in rodent pain models. (2012, November 01). Retrieved March 01, 2018, from https://www.sciencedirect.com/science/article/pii/S0304395912005994?_rdoc=1&_fmt=high&_origin=gateway&_docanchor=&md5=b8429449ccfc9c30159a5f9aeaa92ffb

(26) Murillo-Rodríguez, E., Palomero-Rivero, M., Millán-Aldaco, D., Arias-Carrión, O., & Drucker-Colín, R. (2011, June). Administration of URB597, Oleoylethanolamide or Palmitoylethanolamide Increases Waking and Dopamine in Rats. Retrieved March 01, 2018, from https://www.ncbi.nlm.nih.gov/pmc/articles/PMC3136458/

(27) Tsuboi, K., Takezaki, N., & Ueda, N. (2007, August). The N-acylethanolamine-hydrolyzing acid amidase (NAAA). Retrieved March 01, 2018, from https://www.ncbi.nlm.nih.gov/pubmed/17712833

(28) Migliore, M., Pontis, S., Arriba, A. L., Realini, N., Torrente, E., Armirotti, A., . . . Piomelli, D. (2016, September 05). Second-generation non-covalent NAAA inhibitors are protective in model of multiple sclerosis. Retrieved March 01, 2018, from https://www.ncbi.nlm.nih.gov/pmc/articles/PMC5009002/

(29) Migliore, D. R., Pontis, D. R., Fuentes, A. L., Realini, N., Torrente, E., Armirotti, A., . . . Piomelli, D. (2016, September 05). Second-Generation Non-Covalent NAAA Inhibitors are Protective in a Model of Multiple Sclerosis. Retrieved March 01, 2018, from https://www.ncbi.nlm.nih.gov/pubmed/27404798

(30) Lipina, C., Rastedt, W., Irving, A. J., & Hundal, H. S. (2013, January 25). Endocannabinoids in obesity: brewing up the perfect metabolic storm? Retrieved March 01, 2018, from http://onlinelibrary.wiley.com/doi/10.1002/wmts.79/full

(31) Xue, C., Shirazian, A., Cai, W., Kahn, R., & Pothos, E. (2016, April). The Role of Central Insulin Resistance in Neuronal Synaptic Plasticity Associated with Neuropsychiatric Disorders. Retrieved March 15, 2018, from http://press.endocrine.org/doi/abs/10.1210/endo-meetings.2016.DGM.13.SUN-732

(32) Guglielmo, R., Martinotti, G., Quatrale, M., Ioime, L., Kadilli, I., Nicola, M. D., & Janiri, L. (2015, April 22). Topiramate in Alcohol Use Disorders: Review and Update. Retrieved March 26, 2018, from https://link.springer.com/article/10.1007/s40263-015-0244-0

(33) Johnson, B. A., Roache, J. D., Ait-Daoud, N., Wells, L. T., Wallace, C. L., Dawes, M. A., . . . Wang, X. Q. (2007, February). Effects of acute topiramate dosing on methamphetamine-induced subjective mood. Retrieved March 26, 2018, from https://www.ncbi.nlm.nih.gov/pubmed/16448579

(34) Nirenberg, M. J., & Waters, C. (2006, April). Compulsive eating and weight gain related to dopamine agonist use. Retrieved March 26, 2018, from https://www.ncbi.nlm.nih.gov/pubmed/16261618

(35) Medscape. (2016, December 30). Pramipexole (Rx). Retrieved March 26, 2018, from https://reference.medscape.com/drug/mirapex-mirapex-er-pramipexole-343048#4

(36) Yan, Y., Jiang, W., Liu, L., Wang, X., Ding, C., Tian, Z., & Zhou, R. (2015, January 15). Dopamine controls systemic inflammation through inhibition of NLRP3 inflammasome. Retrieved March 30, 2018, from https://www.ncbi.nlm.nih.gov/pubmed/25594175